Research Paper
J. Astron. Space Sci. 36(1), 1-9 (2019)
https://doi.org/10.5140/JASS.2019.36.1.1

JASS Journal of Astronomy and Space Sciences

Analysis of Field-Aligned Currents in the High-Altitude Nightside Auroral Region: Cluster Observation

Youra Shin[1], Ensang Lee[1,2†], Jae-Jin Lee[3]

[1]School of Space Research, Kyung Hee University, Yongin 17104, Korea
[2]Institute of Natural Sciences, Kyung Hee University, Yongin 17104, Korea
[3]Korea Astronomy and Space Science Institute, Daejeon 34055, Korea

In this paper we present analysis of current density when the Cluster spacecraft pass the nightside auroral region at about 4-5 R_E from the center of Earth. The analysis is made when the inter-spacecraft separation is within 200 km, which allows all four spacecraft to be situated inside the same current sheet. On 22 February 2002, two field-aligned current (FAC) events were observed in both the southern and the northern hemispheres. The FACs were calculated with magnetic field data obtained by the four spacecraft using the Curlometer method. The scales of the FACs along the spacecraft trajectory and the magnitudes were hundreds of kilometers and tens of nA/m^2, respectively, and both events were mapped to the auroral region in the ionosphere. We also examined reliability of the results with some parameters, and found that our results are adequately comparable with other studies. Nevertheless, some limitations that decrease the accuracy of current estimation exist.

Keywords: Field-aligned current, the nightside auroral region, the Curlometer method, Cluster observation

1. INTRODUCTION

Field-aligned currents (FACs) around the auroral regions, also called the Birkeland currents, flow along magnetic field lines into and out of the ionosphere. It is generally accepted that FACs play an important role in the transfer of energy and particles in the solar wind-magnetosphere-ionosphere coupling process. The structure and the generation mechanism of FACs have been one of the most outstanding problems.

Birkeland (1908) first proposed the concept of FACs, and later the transverse magnetic disturbances observed in the auroral region provided the definite evidence for the presence of FACs (Zmuda et al. 1966). It has been reported that in the ionosphere the FACs have large-scale structures: the region 1 (R1) and region 2 (R2) current systems (Iijima & Potemra. 1976a, b, 1978). It was suggested that R2 currents are connected with the partial ring current (Nakano & Iyemori. 2003). The FACs have also been observed in the boundary layer of the inner magnetosphere (Vallet et al. 2005; Zong et al. 2009), the plasma sheet boundary layer (Marklund et al. 2007; Cheng et al. 2011; Nakamura et al. 2016), and the magnetotail (Shi et al. 2010; Cheng et al. 2016). The FACs also exist in the magnetic flux ropes observed in the solar wind (Kim et al. 2017).

FACs are mostly inferred from magnetic field disturbances with a highly time-dependent signature. Because multi-point observations with appropriate configuration are required to accurately measure the currents (Stasiewicz et al. 2000; Lühr et al. 2015), the majority of previous studies have been forced to assume that the structure is time stationary and/or has a simple geometric configuration such as an infinite current sheet. Only recently multi-spacecraft missions such as Cluster, Swarm and MMS have made it possible to estimate the currents less limited by such assumptions. The Cluster (Escoubet et al. 2001) and MMS (Burch et al. 2016) missions are composed of four identical spacecraft, and the Swarm mission (Friis-Christensen et al.

Received 24 DEC 2019 **Revised** 4 MAR 2019 **Accepted** 6 MAR 2019
†**Corresponding Author**
Tel: +82-31-201-2047, E-mail: eslee@khu.ac.kr
ORCID: https://orcid.org/0000-0002-7737-0339

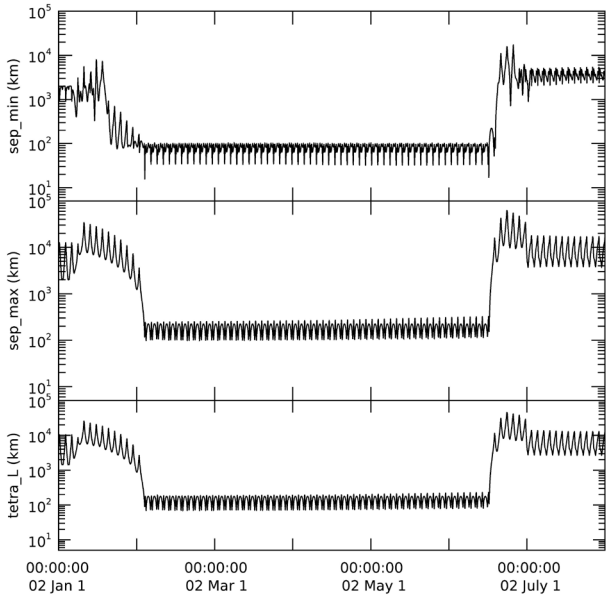

Fig. 1. Minimum (top) and Maximum (middle) inter-spacecraft separation of the four identical spacecraft, and the characteristic size (bottom). The plot shows inter-spacecraft separation and the tetrahedron size of the Cluster spacecraft between January and July in 2002. The separation was maintained within 200 km from February to June in 2002.

2006) has a constellation of three spacecraft.

Cluster, a constellation of four spacecraft, passes the nightside auroral region at the altitude of ~4 – 5 R_E. In that region, magnetic field disturbances, which could be produced by the FACs, are often observed. The magnetic field data measured by the Cluster spacecraft can be used to calculate current density inside a current sheet using the Curlometer method that solves Maxwell-Ampere's law (Dunlop et al. 1988, 2002). In this paper, we use the Curlometer method to estimate FACs observed around the auroral regions in the southern and the northern hemispheres on 22 February 2002. Section 2 and Section 3 introduce data set descriptions and the Curlometer method, respectively. Observations and analysis results are presented in Section 4. Discussion is presented in Section 5, and lastly, a brief summary is given in Section 6.

2. DATA SET DESCRIPTIONS

2.1 Cluster

The Cluster constellation consists of four identical spacecraft, each of which has a polar orbit with a perigee at ~3 R_E and an apogee at ~19 R_E and an orbital period of 57 hours. In summer of the northern hemisphere the perigee locates in the dayside and the Cluster spacecraft cross the dayside polar region. On the other hand, in winter the perigee locates in the nightside and the Cluster spacecraft cross the nightside polar region. Thus, the Cluster spacecraft pass the region above the nightside (dayside) auroral regions of both the southern and the northern hemispheres in winter (summer) of the northern hemisphere. The formation of the Cluster constellation is a tetrahedron structure. Here, we used magnetic field data from the Fluxgate Magnetometer (FGM) instrument (Balogh et al. 2001) on board the Cluster spacecraft. The maximum temporal resolution is 22.5 Hz. In addition, the geomagnetic conditions were obtained from the OMNI data.

2.2 Data

Small separation scale between spacecraft produces good physical linearity of spatial gradients because the linear approximation is generally accurate for small separation. However, as the tetrahedron size becomes smaller than certain threshold, the larger error is induced on the ΔB and the Δr estimation (see Fig. 2 in Robert et al. (1988)). Vallat et al. (2005) suggested that separation by 200 km would allow all four spacecraft to be located within the same current sheet at near perigee. For larger separation distance, the gradients within the tetrahedron would no longer be linear.

To measure current density correctly, therefore, all four spacecraft should be inside the same current distribution, and inter-spacecraft separation distance should be sufficiently small. Fig. 1 shows the minimum (top) and the maximum (middle) inter-spacecraft separation, and the characteristic size (bottom) of the Cluster constellation from January to July in 2002. The separation was maintained within 200 km from February to June in 2002. Thus, during the interval all the spacecraft are likely to be in the same current sheet and the gradients are almost linear, and the configuration is suitable to estimate current density in the nightside auroral region.

3. THE CURLOMETER METHOD

Current density is estimated by applying the Curlometer technique (Dunlop et al. 1988, 2002) with the magnetic field data measured by the four spacecraft. The Curlometer technique directly estimates current density vectors inside the tetrahedron formed by the four spacecraft (see Fig. 1 in Dunlop et al. (2002)). This technique has been used to examine current density in many regions of the magnetosphere.

The main assumptions for the Curlometer technique are as follows. Firstly, the region of interest is stationary, assuming that the field changes much more slowly than

the time scales of the spacecraft motion and linearly inside the tetrahedron. Secondly, spacecraft constellation is considerably regular. Lastly, all measurement points are located within the same current sheet and the current density is almost constant inside the configuration.

This method calculates current density using Maxwell-Ampere's law (Eq. (1)).

$$\vec{J} = \frac{1}{\mu_0} \nabla \times \vec{B} \tag{1}$$

Here, $\vec{J}$ is the current density and μ_0 is the magnetic permeability of free space. In this equation, the displacement current related to the rate of change of the electric field is ignored by assuming steady-state currents. The average current density can be obtained by Eq. (2). Using one spacecraft as the reference, three independent surfaces of the tetrahedron around the reference lead to three equations for its normal vectors, which are the independent components of the average current density.

$$\mu_0 \overrightarrow{J_{av}} \cdot \left(\Delta\vec{r_i} \times \Delta\vec{r_j}\right) = \Delta\overrightarrow{B_i} \cdot \Delta\vec{r_j} - \Delta\overrightarrow{B_j} \cdot \Delta\vec{r_i} \tag{2}$$

Here, $\Delta\vec{r_i}$ is the displacement vector: $\Delta\vec{r_i} = \vec{r_i} - \vec{r}_{reference}$. Also, $\Delta\vec{B_i}$ is the difference of the magnetic fields between the ith and the reference spacecraft, defined as $\Delta\vec{B_i} = \vec{B_i} - \vec{B}_{reference}$. For example, considering that spacecraft C1, C2 and C3 form a surface and C3 is the reference spacecraft, Eq. (2) can be written as Eq. (3), where $\Delta\overrightarrow{r_{13}}$ is the displacement between C1 and C3 and $\Delta\overrightarrow{B_{13}}$ is the difference of magnetic fields at C1 and C3. From Eq. (3), we can estimate the average current density flowing through the surface, $\overrightarrow{J_{123}}$.

$$\mu_0 \overrightarrow{J_{123}} \cdot (\Delta\overrightarrow{r_{13}} \times \Delta\overrightarrow{r_{23}}) = \Delta\overrightarrow{B_{13}} \cdot \Delta\overrightarrow{r_{23}} - \Delta\overrightarrow{B_{23}} \cdot \Delta\overrightarrow{r_{13}} \tag{3}$$

Then, the average current density, $\overrightarrow{J_{13}}$, can be determined by the average current densities on three adjacent surfaces of the tetrahedron, $\overrightarrow{J_{123}}$, $\overrightarrow{J_{134}}$, and $\overrightarrow{J_{234}}$, centered at C3. In this method, the current calculation is not significantly influenced by selecting a spacecraft as a reference (Vallat et al. 2005).

4. OBSERVATIONS AND RESULTS

Cluster detected currents for most of the orbits between February and June in 2002 although the intensity is small in some cases. In this study, we analyzed an event observed on 22 February 2002 in detail, for which remarkable current densities were observed in both hemispheres.

The event occurred in the southern and the northern hemispheres at ~14:49 UT and ~17:17 UT, respectively, on 22 February 2002. Fig. 2 shows the trajectories of the Cluster spacecraft projected on (a) the X-Y plane and (b) the X-Z plane in the Geocentric Solar Ecliptic (GSE) coordinates. Black lines are for the trajectory of the Cluster spacecraft from 13:00 UT to 19:00 UT, moving from the southern to the northern hemispheres in the nightside, and red lines represent the parts of the trajectory where large current densities were observed. Fig. 3 represents inter-spacecraft separation for the two events using C3 as a reference on the ΔX-ΔY plane (upper) and the ΔX-ΔZ plane (lower) in (a) the southern and (b) the northern hemispheres, which show that all four spacecraft were within around 200 km from each other.

Fig. 4 represents geomagnetic conditions on 22 February 2002: from top to bottom shown are the AE, Kp and SYM/H indices. Two vertical lines mark the time when the events occurred. Each event occurred when the AE index was 78 and 106 nT. The Kp index was 1-2, and the SYM/H index

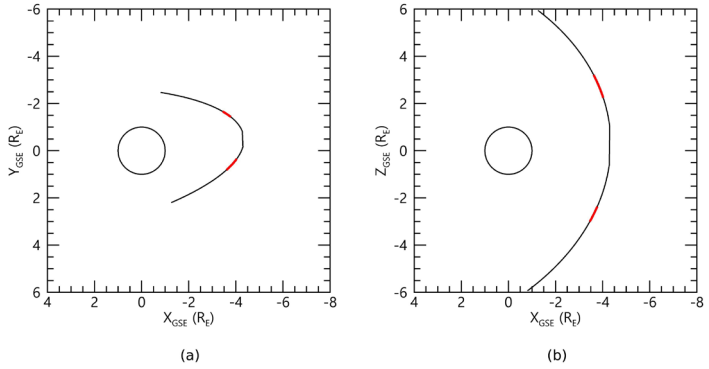

Fig. 2. Trajectories of the Cluster spacecraft projected on (a) the X-Y plane and (b) the X-Z plane in the GSE coordinates. Black lines are for the trajectory of the Cluster spacecraft from 13:00 UT to 19:00 UT, moving from the southern to the northern hemispheres in the nightside, and red lines represent the parts of the trajectory where large current densities were observed.

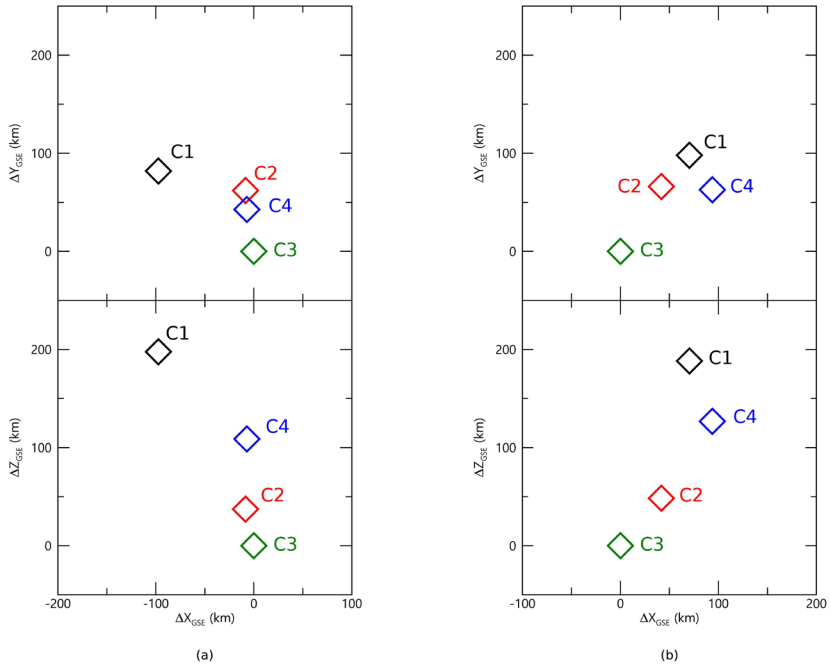

Fig. 3. Inter-spacecraft separation for the two events using C3 as a reference on the ΔX-ΔY plane (upper) and the ΔX-ΔZ plane (lower) in (a) the southern and (b) the northern hemispheres. This plot suggested that all four spacecraft were within around 200 km from each other.

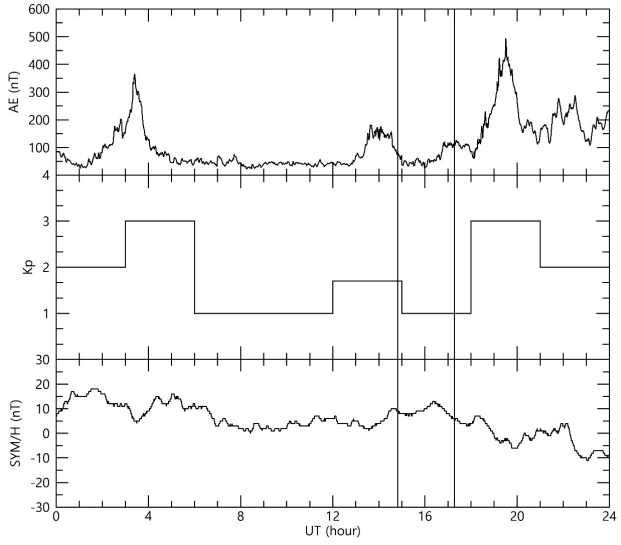

Fig. 4. Geomagnetic conditions on 22 February 2002: from top to bottom shown are the AE, Kp and SYM/H indices. Two vertical lines mark the time when the events occurred. Each event occurred when the AE index was 78 and 106 nT. The Kp index was 1-2, and the SYM/H index was 9 and 6 nT, only very weakly fluctuating around zero for several days (not shown in this paper). All these indicate that geomagnetic activity was very quiet during the events.

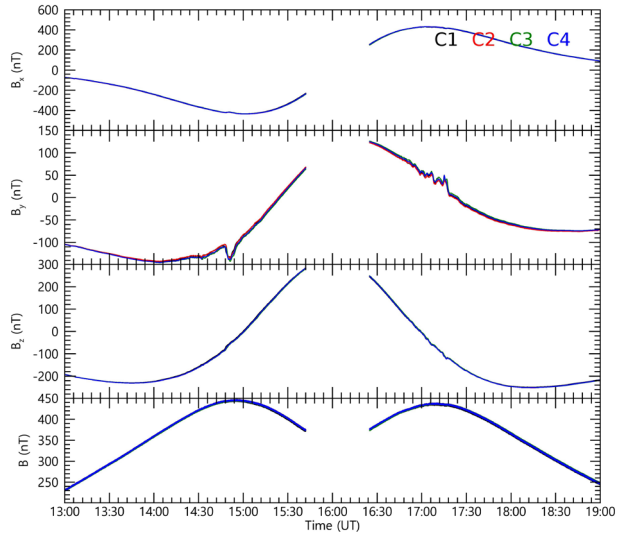

Fig. 5. From top to bottom, three components of the magnetic field in the GSE coordinates observed by the four spacecraft and the total magnitude. The magnetic field was observed from 13:00 UT to 19:00 UT when the Cluster spacecraft passed from the southern to the northern polar regions in the nightside. In our study, the 5 Hz resolution data was averaged to 3 second resolution; there was no data between 15:44 UT and 16:23 UT. Two prominent magnetic disturbances, especially in the B_y component, were observed at 14:49 UT and 17:17 UT as Cluster passed the auroral regions in the southern and the northern hemispheres, respectively.

was 9 and 6 nT, only very weakly fluctuating around zero for several days (not shown in this paper). All these indicate that geomagnetic activity was very quiet during the events.

The magnetic field was observed from 13:00 UT to 19:00 UT when the Cluster spacecraft passed from the southern to the northern polar regions in the nightside as shown in Fig. 5. In our study, the 5 Hz resolution data was averaged to 3 second resolution. Note that there was no data between 15:44 UT and 16:23 UT. The top three panels represent three components of the magnetic field in the

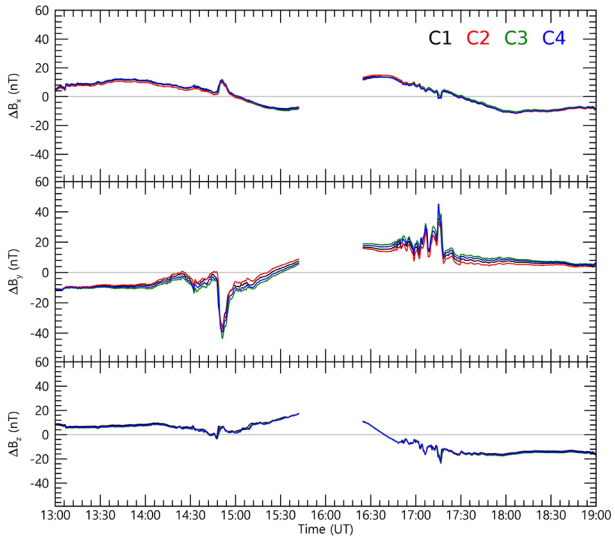

Fig. 6. From top to bottom, three components of observed the magnetic field subtracted by TS04 model. Slight difference is seen in each component due to discrepancy between the observed and model values.

GSE coordinates observed by the four spacecraft, and the last panel represents the total magnitude. Two prominent magnetic disturbances, especially in the B_y component, were observed at 14:49 UT and 17:17 UT as Cluster passed the auroral regions in the southern and the northern hemispheres, respectively. The observed magnetic field was subtracted by the magnetic field obtained from the Tsyganenko model (TS04 model) (Tsyganenko & Sitnov. 2005), which is presented in Fig. 6. In each component there exists slight difference between the observed and model values even when there is no disturbance, which causes the reference line not exactly zero, but the difference can be ignored because only the difference between spacecraft affects the current estimation in the Curlometer method.

Fig. 7 shows the results of the current estimation for the two events in both hemispheres. First of all, the average magnetic disturbance from the four measurements by the Cluster spacecraft in the southern hemisphere is

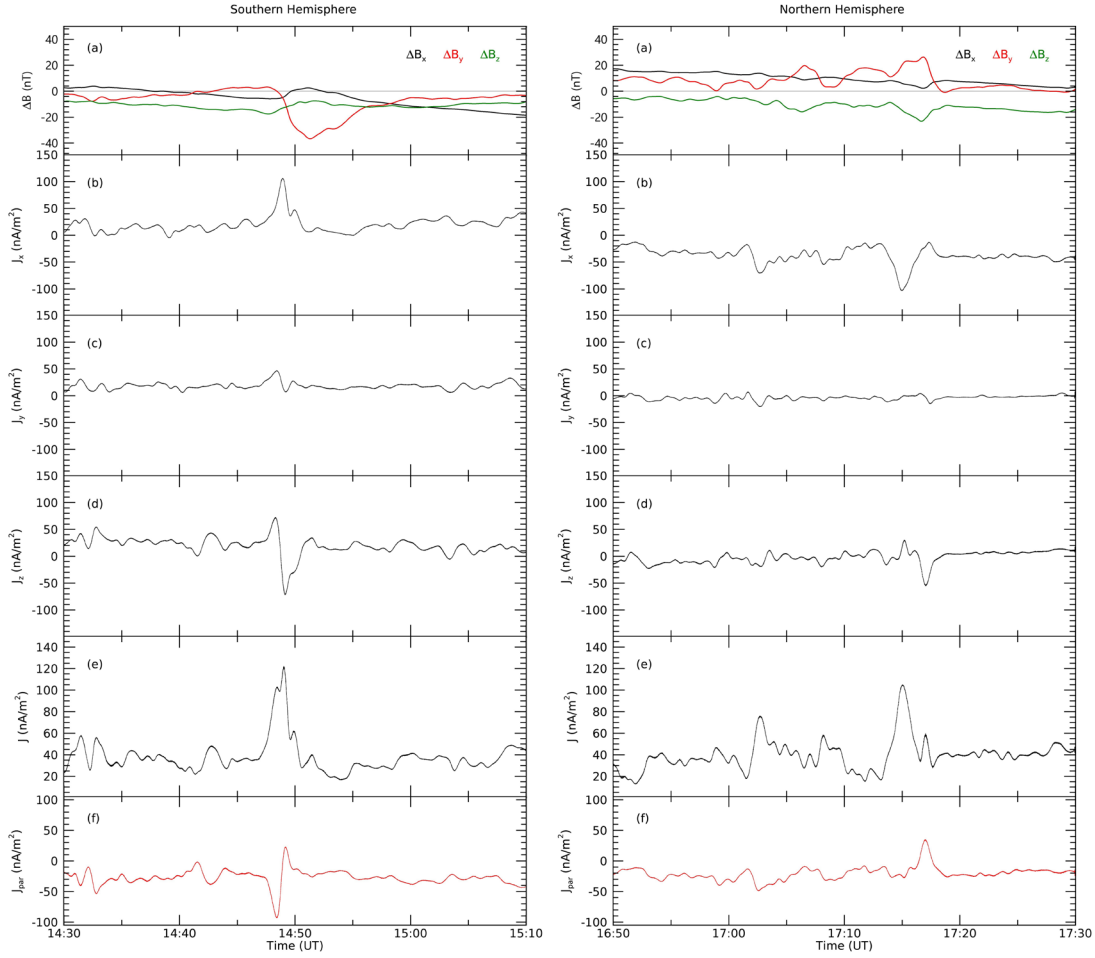

Fig. 7. Results of the current estimation for the two events in the southern hemisphere (left) and the northern hemisphere (right). From top to bottom: (a) the average magnetic disturbance from the four measurements by the Cluster spacecraft; (b), (c) and (d) three components of the calculated current density; (e) the total magnitude of the current density; (f) the parallel component of the current density.

approximately 40 nT, which is mainly generated by the B_y component seen in the top panel (a). In the following panels, the x, y and z components and the total magnitude of the calculated current density are shown. In the bottom panel (f), the parallel component of the current density is presented, which shows a bipolar signature with a minimum at 14:48 UT and a maximum at 14:49 UT. This indicates that double FAC sheets were formed. The FAC is collocated with the variation of the current components, which corresponds to the location where the magnetic field is mostly changing. The valley of the bipolar FAC signature, which is associated with downward (earthward) current, is mapped to the invariant latitude of ~64.0° in the ionosphere. On the other hand, the peak, which is associated with upward (tailward) current, is mapped to ~63.8°. The scale of the FAC along the spacecraft trajectory was 516 km from the valley to the peak and the magnitude was 70.04 nA/m^2 at the valley and 46.70 nA/m^2 at the peak.

The averaged magnetic disturbance in the northern hemisphere consists of small-amplitude fluctuations in the entire period, but, nevertheless, possesses a distinct peak. It also chiefly occurred in the B_y component as shown in the first panel (a). The bottom panel (f) shows that the FAC has a monopolar signature with a positive peak at 17:17 UT, and is fairly collocated with variation of the J_z component and a drastic change of the magnetic field, but not with the J_x component and the total magnitude. The latter corresponds to variation of the perpendicular component of the current (not shown here), which will be discussed in Section 5. This peak is mapped to the invariant latitude of ~64.2° in the ionosphere, where the signature is associated with downward (earthward) current. The scale of the FAC along the spacecraft trajectory was 805 km and the magnitude was 56.76 nA/m^2.

5. DISCUSSION

The two FAC events were observed on 22 February 2002 in both the southern and the northern hemispheres. In the southern hemisphere, the FAC had a bipolar signature, implying that double FAC sheets were formed. Each sheet is traced to the ionosphere at the invariant latitudes of ~64.0° and ~63.8°. This structure is located at the post-midnight sector around 01 Magnetic Local Time (MLT). The bipolar FACs correspond to downward and upward currents, respectively. In the northern hemisphere, a monopolar FAC signature is observed, which is traced to the ionosphere at the invariant latitude of ~64.2°. MLT is near midnight in the post-midnight sector, and the FAC corresponds to downward current. Accordingly, this monopolar FAC structure correlates to the R1 current in the post-midnight sector. However, it is mapped to the invariant latitude lower than that reported by Ijima & Potemra (1976a), in which the R1 currents are located at the invariant latitudes between 70° and 75° in the northern hemisphere during a quiet time. In addition, Ren et al. (2016) reported using statistical analysis that in the same region as in this study, current density is tens of nA/m^2, the thickness is hundreds of kilometers, and the distribution of FACs in magnetic latitude mapped to the ionosphere coincides with the auroral zone. These results are well consistent with our results.

In Fig. 4, each event occurred when the AE index was 78 and 106 nT and the Kp index was 1-2. It is comparable with the work by Ren et al. (2016), in which the relations between J (ΔB) and the indices (AE and Kp) were determined using the linear fits in the same region as in this study. The relations are (1) J (FAC) = 39.62+0.01×AE, J (FAC) = 15.20+13.09×Kp, and (2) ΔB = 24.62+0.04×AE, ΔB = 18.02+8.38×Kp. In the southern hemisphere, the values of the FAC and the ΔB estimated in this study are 70.04 nA/m^2 and 29.47 nT, respectively, and in the northern hemisphere, 56.76 nA/m^2 and 36.91 nT, respectively. The results from the relations based on AE by Ren et al. (2016) indicate 40.4 nA/m^2 and 27.74 nT in the southern hemisphere, and 40.68 nA/m^2 and 28.86 nT in the northern hemisphere. The results from the relations based on Kp result in 37.45 nA/m^2 and 23.27 nT in the southern hemisphere, and 28.29 nA/m^2 and 26.4 nT in the northern hemisphere. These show that both the magnitudes of the FAC density and the ΔB measured in this study are greater than the values from the statistical results by Ren et al. (2016) for both hemispheres.

We examined how reliable the current estimation is in

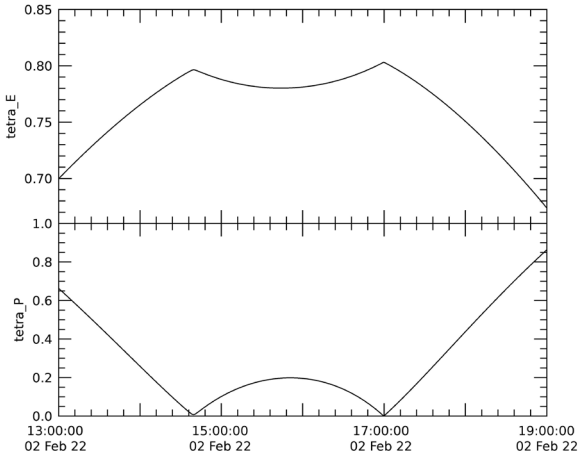

Fig. 8. Two parameters with respect to the Cluster configuration with elongation (upper) and planarity (lower) from 13:00 UT to 19:00 UT on 22 February 2002 when the Cluster spacecraft passed from the southern to the northern polar regions in the nightside. These parameters define the shape of the Cluster constellation for both events.

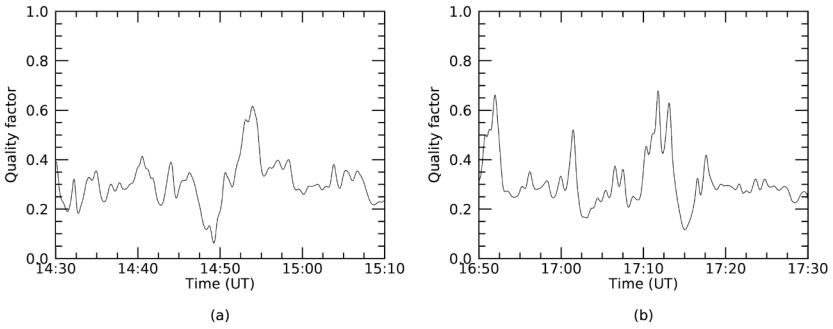

Fig. 9. Quality factor, $|\nabla\cdot\vec{B}|/|\nabla\times\vec{B}|$, in (a) the southern hemisphere and (b) the northern hemisphere. This is an indicator of the uncertainty in the current estimation. The Quality factor in this study is ~0.3 in average for both events, and the parts that are abruptly increased can be explained by sudden change between the magnetic field magnitudes related to the increase in elongation of the tetrahedron (Grimald et al. 2012).

terms of some parameters. Fig. 8 shows two parameters with respect to the Cluster configuration with elongation (upper) and planarity (lower) from 13:00 UT to 19:00 UT on 22 February 2002 when the Cluster spacecraft passed from the southern to the northern polar regions in the nightside. These parameters define the shape of the Cluster constellation for both events. The values of the elongation and the planarity are 0.792696 and 0.0493406, respectively, in the southern hemisphere and 0.791371 and 0.115107, respectively, in the northern hemisphere. The uncertainty, therefore, for both events is not larger than 20 % (Robert et al. 1998). In addition, as shown in Fig. 3, the four spacecraft are largely elongated along the Z-axis. Because the tetrahedron is elongated along the Z-axis, the error on the estimation of $\vec{J}$ would mostly be carried by the J_z component, which is described by the gradients in the X and Y directions (Vallat et al. 2005).

Quality factor, $|\nabla\cdot\vec{B}|/|\nabla\times\vec{B}|$, is also an indicator of the uncertainty in the current estimation. It is generally accepted that the desirable values of this indicator are $\ll 1$ (Haaland et al. 2004). Dunlop et al. (2015) and Cheng et al. (2016) also suggested that the values should be < 0.3 to ensure the quality of the current estimation. In Fig. 9, quality factor in this study is ~0.3 in average for both events, which is just the threshold as suggested in the previous studies. The parts of the quality factor that are abruptly increased can be explained by sudden change between the magnetic field magnitudes related to the increase in elongation of the tetrahedron (Grimald et al. 2012).

The current structures observed in this study have the temporal extent shorter than a minute. Because the speed of the Cluster spacecraft is 4-5 km/s at around perigee, the current structures would have the width smaller than ~300 km. These narrow current structures inevitably include nonlinear magnetic field gradients inside the tetrahedron because not all spacecraft are simultaneously located in the same current sheet (Vallat et al. 2005). This causes the increase of estimation error.

In general there is much small-scale perturbation in the calculated current density. Such a localized filamentary current structure is thought to be driven by Alfven waves (Stasiewicz et al. 2000). In addition, FACs, in a more dynamic nature, can develop when magnetospherically generated Alfven waves propagate through the ionosphere and interact with the ionosphere. Therefore, it is important to be able to distinguish the ΔB generated by a current sheet from the ΔB by an Alfven wave. In this point of view, the physical process needs to be further studied.

6. SUMMARY

The two FAC events were observed in the nightside auroral region at about 4-5 R_E from the center of Earth in both the southern and the northern hemispheres on 22 February 2002. The current densities were estimated with the magnetic field data obtained by the four spacecraft using the Curlometer method. During the events, geomagnetic activity was very quiet. In the southern hemisphere, the valley of the bipolar FAC signature, which is associated with downward (earthward) current, is mapped to the invariant latitude of ~64.0° in the ionosphere. On the other hand, the peak, which is associated with upward (tailward) current, is mapped to ~63.8°. The scale of the FAC along the spacecraft trajectory was 516 km from the valley to the peak and the magnitude was 70.04 nA/m^2 at the valley and 46.70 nA/m^2 at the peak. In the northern hemisphere, the peak of the monopolar FAC signature is mapped to the invariant latitude of ~64.2° in the ionosphere, where the signature is associated with downward (earthward) current. The scale

of the FAC along the spacecraft trajectory was 805 km and the magnitude was 56.76 nA/m^2. Our results adequately correspond to other works (Iijima & Potemra 1976a, b; Vallat et al. 2005; Dunlop et al. 2015; Cheng et al. 2016; Ren et al. 2016) but some parameters that decrease the accuracy of current estimation exist. The limitations in terms of the physical process mentioned above need to be further studied.

ACKNOWLEDGEMENTS

This work was partly supported by the BK21Plus Program and the Space Core Technology Development Program through the NRF of Korea funded by Ministry of Science and ICT (NRF-2017M1A3A3A02016781). This work was also partly supported by the Korea Astronomy and Space Science Institute under the R&D program in 2017 supervised by the Ministry of Science and ICT.

REFERENCES

Balogh A, Carr CM, Acuna MH, Dunlop MW, Beek TJ, et al., The Cluster Magnetic Field Investigation: overview of in-flight performance and initial results, Ann. Geophys. 19, 1207-1217 (2001). https://doi.org/10.5194/angeo-19-1207-2001

Birkeland K, The Norwegian Aurora Polaris Expedition (H. Aschehoug & Co., Christiania, 1908).

Burch JL, Moore TE, Torbert RB, Giles BL, Magnetospheric multiscale overview and science objectives, Space Sci. Rev. 199, 5-21 (2016). https://doi.org/10.1007/s11214-015-0164-9

Cheng ZW, Shi JK, Zhang TL, Wang SG, Liu ZX, Field-Aligned Currents at the PSBL on 17 August 2001 Storm: Relationships with solar Wind Conditions, Chin. Phys. Lett. 28, 099401 (2011). https://doi.org/10.1088/0256-307X/28/9/099401

Cheng ZW, Zhang JC, Shi JK, Kistler LM, Dunlop M, et al., The particle carriers of field-aligned currents in the Earth's magnetotail during a substorm, J. Geophys. Res. Space Phys. 121, 3058-3068 (2016). https://doi.org/10.1002/2015JA022071

Dunlop MW, Southwood DJ, Glassmeier KH, Neubauer FM, Analysis of multipoint magnetometer data, Adv. Space Res. 8, 273-277 (1988). https://doi.org/10.1016/0273-1177(88)90141-X

Dunlop MW, Balogh A, Glassmeier KH, Robert P, Four-point Cluster application of magnetic field analysis tools: The Curlometer, J. Geophys. Res. 107, 1384 (2002). https://doi.org/10.1029/2001JA005088

Dunlop MW, Yang YY, Yang JY, Lühr H, Shen C, et al., Multispacecraft current estimates at swam, J. Geophys. Res. Space Phys. 120, 8307-8316 (2015). https://doi.org/10.1002/2015JA021707

Escoubet CP, Fehringer M, Goldstein M, *Introduction* The Cluster mission, Ann. Geophys. 19, 1197-1200 (2001). https://doi.org/10.5194/angeo-19-1197-2001

Friis-Christensen E, Lühr H, Hulot G, Swarm: A constellation to study the Earth's magnetic field, Earth, Planets and Space. 58, 351-358 (2006). https://doi.org/10.1186/BF03351933

Grimald S, Dandouras I, Robert P, Lucek E, Study of the applicability of the curlometer technique with the four Cluster spacecraft in regions close to Earth, Ann. Geophys. 30, 597-611 (2012). https://doi.org/10.5194/angeo-30-597-2012

Haaland S, Sonnerup BUO, Dunlop MW, Georgescu E, Paschmann G, et al., Orientation and motion of a discontinuity from Cluster curlometer capability: Minimum variance of current density, Geophys. Res. Lett. 31, L10804 (2004). https://doi.org/10.1029/2004GL020001

Iijima T, Potemra TA, The amplitude distribution of field-aligned currents at northern high latitudes observed by Triad, J. Geophys. Res. 81, 2165-2174 (1976a). https://doi.org/10.1029/JA081i013p02165

Iijima T, Potemra TA, Field-Aligned Currents in the Dayside Cusp Observed by Triad, J. Geophys. Res. 81, 5971-5979 (1976b). https://doi.org/10.1029/JA081i034p05971

Iijima T, Potemra TA, Large-Scale Characteristics of Field-Aligned Currents Associated With Substroms, J. Geophys. Res. 83, 599-615 (1978). https://doi.org/10.1029/JA083iA02p00599

Kim MJ, Park KS, Lee DY, Choi CR, Kim RS, et al., Characteristics and geoeffectiveness of small-scale magnetic flux ropes in the solar wind, J. Astron. Space Sci. 34, 237-244 (2017). https://doi.org/10.5140/JASS.2017.34.4.237

Luhr H, Park J, Gjerloev JW, Rauberg J, Michaelis I, et al., Field-aligned currents' scale analysis performed with the Swarm constellation, Geophys. Res. Lett. 42, 1-8 (2015). https://doi.org/10.1002/2014GL062453

Marklund G, Johansson T, Lileo S, Karlsson T, Cluster observations of an auroral potential and associated field-aligned current reconfiguration during thinning of the plasma sheet boundary layer, J. Geophys. Res. 112, A01208 (2007). https://doi.org/10.1029/2006JA011804

Nakamura R, Sergeev VA, Baumjohann W, Plaschke F, Magnes W, et al., Transient, small-scale field-aligend currents in the plasma sheet boundary layer during storm time substorms, Geophys. Res. Lett. 43, 4841-4849 (2016). https://doi.org/10.1002/2016GL068768

Nakano S, Iyemori T, Local time distribution of net field-aligned currents derived from high-altitude satellite data, J. Geophys. Res. 108, 1314 (2003). https://doi.org/10.1029/2002JA009519

Ren J, Zong QG, Zhou XZ, Zhang H, Fu SY, et al., Statistics of the field-aligned currents at the high-latitude energetic electron boundaries in the nightside: Cluster observation, J. Geophys. Res. Space Phys. 121, 1979-1989 (2016). https://doi.org/10.1002/2015JA021754

Robert P, Dunlop MW, Roux A, Chanteur G, Accuracy of Current Density Determination, ISSI Scientific Report SR-001, 395-418 (1998).

Shi JK, Cheng ZW, Zhang TL, Dunlop M, Liu ZX, et al., South-north asymmetry of field-aligned currents in the magnetotail observed by Cluster, J. Geophys. Res. 115, A07228 (2010). https://doi.org/10.1029/2009JA014446

Stasiewicz K, Bellan P, Chaston C, Kletzing C, Lysak R, et al., SMALL SCALE ALFVENIC STURCTURE IN THE AURORA, Space Sci. Rev. 92, 423-533 (2000). https://doi.org/10.1023/A:100520720

Tsyganenko NA, Sitnov MI, Modeling the dynamics of the inner magnetosphere during strong geomagnetic storms, J. Geophys. Res. 110, A03208 (2005). https://doi.org/10.1029/2004JA010798

Vallat C, Dandouras I, Dunlop M, Balogh A, Lucek E, et al., First current density measurements in the ring current region using simultaneous multi-spacecraft CLUSTER-FGM data, Ann. Geophys. 23, 1849-1865 (2005). https://doi.org/10.5194/angeo-23-1849-2005

Zmuda AJ, Martin JH, Heuring FT, Transverse magnetic disturbances at 1100 Kilometers in the auroral region, J. Geophys. Res. 71, 5033-5045 (1966). https://doi.org/10.1029/JZ071i021p05033

Zong QG, Wang YF, Yang B, Zhang H, Tian AM et al., Vortex-like plasma flow structures observed by Cluster at the boundary of the outer radiation belt and ring current: A link between the inner and outer magnetosphere, J. Geophys. Res. 114, A10211 (2009). https://doi.org/10.1029/2009JA014388